Petroleum and Coal

Article Open Access

Well Log Analysis and Reservoir Characterisation of Ronier 6-1 Well in the Bongor Sedimentary Basin

Mahamat Choukou Mahamat[1], *Matthew E. Nton*[2], *Mahamat Nour Abdallah*[3], *Justin Protais Bekono Ottou*[4]

[1] *Pan African University, Institute of Life and Earth Sciences Institute (Including Health and Agriculture), Ibadan, Oyo State, Nigeria*
[2] *Department of Geology, University of Ibadan, Ibadan, Nigeria*
[3] *Department of Geology, Laboratory Hydro-Geosciences and Reservoirs, University of Ndjamena, Chad*
[4] *Department of Earth Science, University of Yaounde I, Yaounde, Cameroon*

Received February 12, 2025; Accepted May 21, 2025

Abstract

The paper presents a comprehensive study of the Ronier oil field located within the Bongor sedimentary Basin of Chad, a region of significant hydrocarbon exploration activity in Central Africa. The primary objective of this research is to delineate and characterize hydrocarbon-bearing reservoirs encountered in the Ronier 6-1 well. Through the meticulous analysis of various well logs, including gamma-ray, resistivity, neutron, and density logs, this study aims to derive critical insights into reservoir lithology and associated petrophysical properties such as porosity and permeability.

Schlumberger Petrel software was employed for the processing, visualization, and analysis of various well logs. Gamma ray, neutron, density, and VCL_HILT (shale volume) logs were used to determine that all 31 identified reservoirs are highly shaly sandstone reservoirs, containing over 30% clay volume. Among these 31 reservoirs, only 6 (Reservoirs 3, 5, 7, 8, 10, and 25) exhibited fair potential. Reservoirs 3, 7, and 8 have a porosity of 20%, while Reservoirs 5, 10, and 25 have a porosity of 19%. Hydrocarbon saturations range from 24% (Reservoir 25) to 55% (Reservoir 8). Irreducible water saturation is highest in Reservoir 25 at 49% and lowest in Reservoir 8 at 30%. These 6 reservoirs exhibit good permeability, with values ranging from 31.44 mD (Reservoir 8) to 9.46 mD (Reservoir 25). Reservoir 25 is the thickest with approximately 11.65 m of gross pay thickness and 6.15 m of net pay thickness. The thinnest reservoir among the six is Reservoir 8, which is approximately 2.06 m thick.

Keywords: *Bongor basin; Ronier oilfield; Well log analysis; Reservoir characterization; Hydrocarbon potential.*

1. Introduction

The Bongor Basin of Chad is one of the geological provinces of strategic importance for the exploration and exploitation of hydrocarbons in Central Africa [1]. The basin covers an area of approximately 18,000 km^2 (Figure 2). It was formed following a series of complex tectonic processes, including rifting movements that have formed its distinctive geological architecture [2-3]. Log analysis and reservoir characterisation are integral parts of hydrocarbon exploration and production processes [4]. Wireline logging aims to investigate the borehole using different methods (resistivity, gamma ray, etc.) to detect and characterise potential hydrocarbon Reservoirs [5-6].

Due to its growing importance in the petroleum industry, this basin is receiving increasing attention, and studies are being conducted to better understand its geological settings and hydrocarbon reservoirs. The focus of this study is the characterisation of the Ronier 6-1 hydrocarbon reservoirs using well log analysis. The objective is to identify and characterise all the potential hydrocarbon reservoirs, then extract the oil reservoirs whose qualities are at least fair. Before doing so, it would be interesting to understand the geological settings of the Bongor sedimentary basin. Then, we will present and discuss the different results.

2. Geological setting

2.1. Tectonic setting and location

The Bongor Basin is described as a passive intracontinental rift basin located within the southwestern corner of Chad on the convergence area of the West and Central African Rift System (WCARS). With an area of approximately 18,000 km2, it includes several studies [2, 7-8]. Then, it was resulted from the extensional movement of the Central African Shearing Zone (CASZ) within the dextral shear stress field on the southern boundary of the Saharan Metacraton [3,9]. Southward, the basin is separated from the Doba-Doseo Basin by a basement high [10].

The Bongor Basin, a miniature NW-SE trending half-graben with spindle-shaped, planar geometry, is mainly composed of the North Slope Belt, the Central Depression, the South Uplift, and the South Depression. According to Zhao *et al.* [11] (Figure 2), the Bongor Basin went through several tectonic phases, three of which were rifting events and two were inversion events.

It is during Early Cretaceous time that the CASZ was fully activated as a part of a fully rifting segment of the aulacogen entering the African continent, generating a series of rift basin groups, and then slowly waned after complete detachment of African from South American plates [1,12].

It was during the N-S Santonian Compressional Event (85-80Ma±), which occurred during the Late Cretaceous period that the Bongor, Doba, Doseo, and Salamat Basin groups were divided into four independent parts (Figure 2) [13]. This then gradually went into the post-rift phase, interrupted by a primary compressive event created toward the end of the Oligocene due to the NE-SW extension of the Red Sea [14-15].

2.2. Stratigraphy

The rocks and sediments under the Bongor Basin mainly come from two sources. First, there are very old rocks from the Late Proterozoic time, which were changed by heat and pressure (metamorphic) or formed from molten material (magmatic) during the Pan-African event [10,16-17]. Second, there are large amounts of sediments from the Cretaceous period, which make up most of the material filling the basin (Figure 1). These sediments can be as thick as 9 kilometers [7].

The upper layers of the Cretaceous rocks are mostly missing, and the lower layers were worn away because of the collision between the African and Eurasian plates during the Santonian stage [2]. This collision caused a lot of erosion, removing more than one kilometer of material on average. The remaining lower Cretaceous rocks include formations called Prosopis, Mimosa, Kubla, Ronier, and Baobab (Figure 1) [18].

The Prosopis and Mimosa Formations are made up of layers of underwater fan and fan-delta deposits mixed with deep lake dark mudstones and shales [11]. The Kubla Formation includes fan-delta, braided-river-delta, and shallow-lake mudstone sections, which are made of sandstones and pebble layers mixed with silty mudstones and grayish-black basalt. The Ronier Formation is known for its river-delta sandstones mixed with shallow gray lake mudstones. The Baobab Formation, as noted by Dou *et al.* [3], is entirely made of river-plain deposits, such as mixed-colored (pebbly) sands and muds (Figure 1).

The Lower Cretaceous layer is the thickest in the Bongor Basin, reaching up to 10 km. There is a lot of debate about whether the Upper Cretaceous layer was also deposited in this basin. However, other nearby basins, like the Doba-Doseo Basin and the Benue Trough, have very thick Upper Cretaceous sediments [19]. In the Muglad Basin in Sudan, the Melut Basin in South Sudan, and other basins in the region, the Upper Cretaceous sediments sit directly on top of the solid Lower Cretaceous layer. This is supported by evidence of parallel unconformities between the layers and angular unconformities at the edges of the rift basins [20].

During the late Early Cretaceous period, this basin was compressed by about 8%. Because of this, it is estimated that around 500-2000 meters (about 1640-6560 feet) of rock from the

Cretaceous and Paleogene periods has been worn away [3]. Later, during the Neogene and Quaternary periods, loose sand and shale layers, about 200-500 meters (around 656-1640 feet) thick, were deposited over the older Lower Cretaceous rocks, but not evenly. So far, more than 10 oil and gas fields have been found in the Lower Cretaceous sandstone layers [18] (Figure 1).

According to Dou *et al.* [21-22], the shale layers in the Prosopis and Mimosa formations contain a lot of organic material, specifically types I-II1 kerogen. These shales have an average Total Organic Carbon (TOC) value of about 3.5%, which makes them key source rocks for oil and gas. Oil and gas have been found in the Lower Cretaceous layers and in the fractured Precambrian basement [3,21,23].

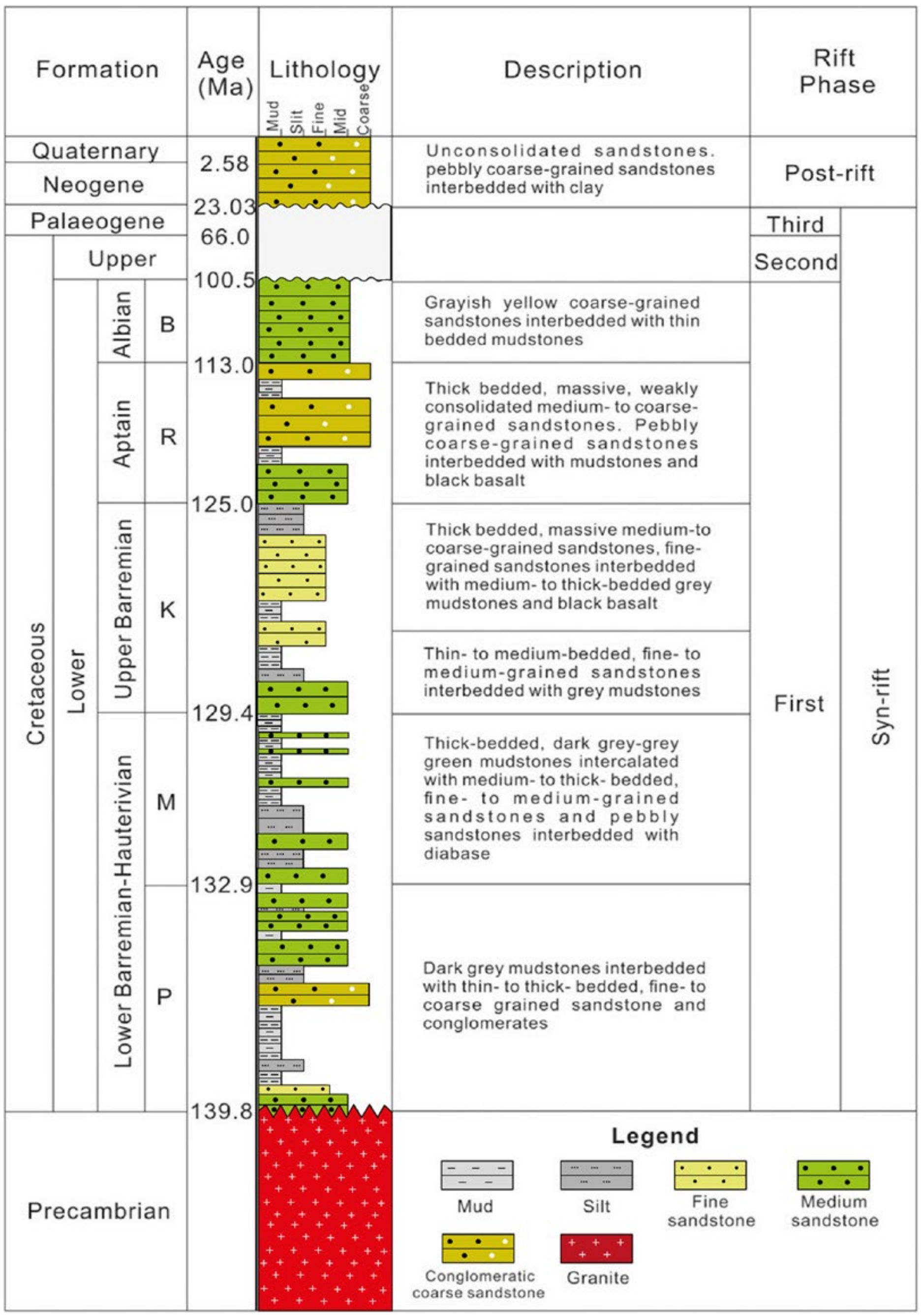

Figure 1. Simplified rock layers and tectonic characteristics of the Lower Cretaceous strata in the Bongor Basin, Chad (modified from [3,7,13,18,24]).

3. Materials and methods

The Ronier oil field is located in the Bongor sedimentary basin, in Chad (Figure 2). This study mostly relied on the available well log data of Ronier 6-1 oil well (Figure 3). The Centre of Petroleum Documentation (CPD) of the Ministry of Petroleum (Chad Republic) provided those data. The Schlumberger's software Petrel was used to visualise, process and analyse the well logs data. The following rock properties were calculated for each identified hydrocarbon reservoir: shale volume (Vsh), effective porosity (Ø), permeability (K), water saturation (S_w), irreducible water saturation (S_{wirr}) and hydrocarbon saturation (S_h).

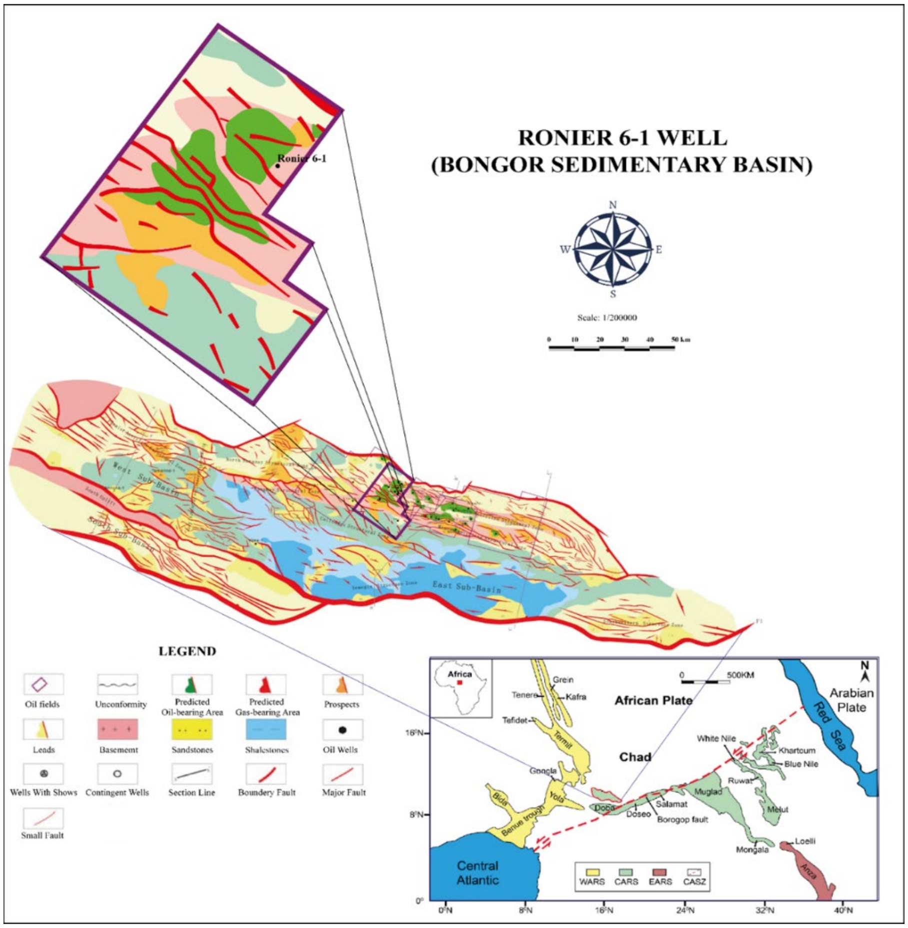

Figure 2. Location of the Ronier 6-1 well in the Bongor sedimentary basin. WARS: West African Rift System; CARS: Central African Rift System; EARS: East African Rift System; CASZ: Central African Shear Zone. (modified from [25]).

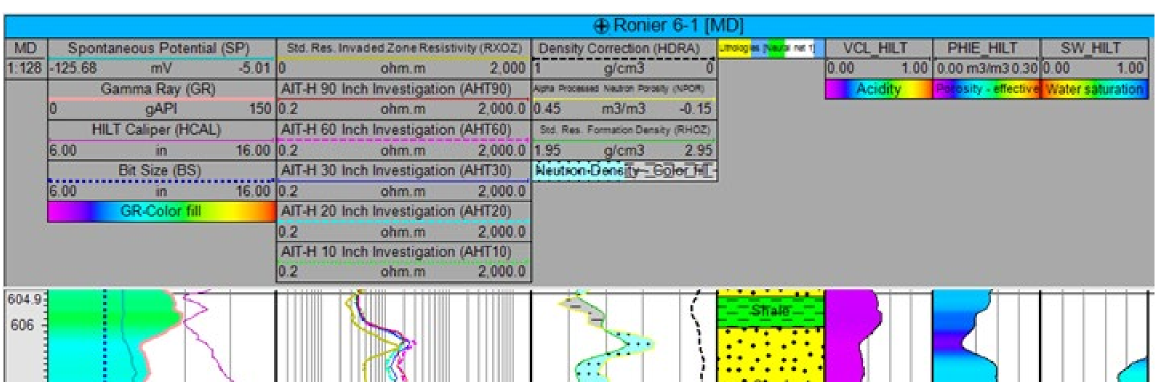

Figure 3. Cross-section header showing some well logs used in this study.

3.1. Lithology determination

Gamma ray, neutron, density, and spontaneous potential (SP) logs were utilized to determine various lithologies. Initially, a manual interpretation was conducted. Subsequently, the Neural Net functionality within the Petrel software was employed (Figure 4). This Neural Net feature leverages the manual interpretation, in conjunction with additional logs (gamma ray, neutron, etc.), to automatically determine lithologies for the remaining geological layers. The accuracy and comprehensiveness of the manual interpretation directly influence the precision of the Neural Network results.

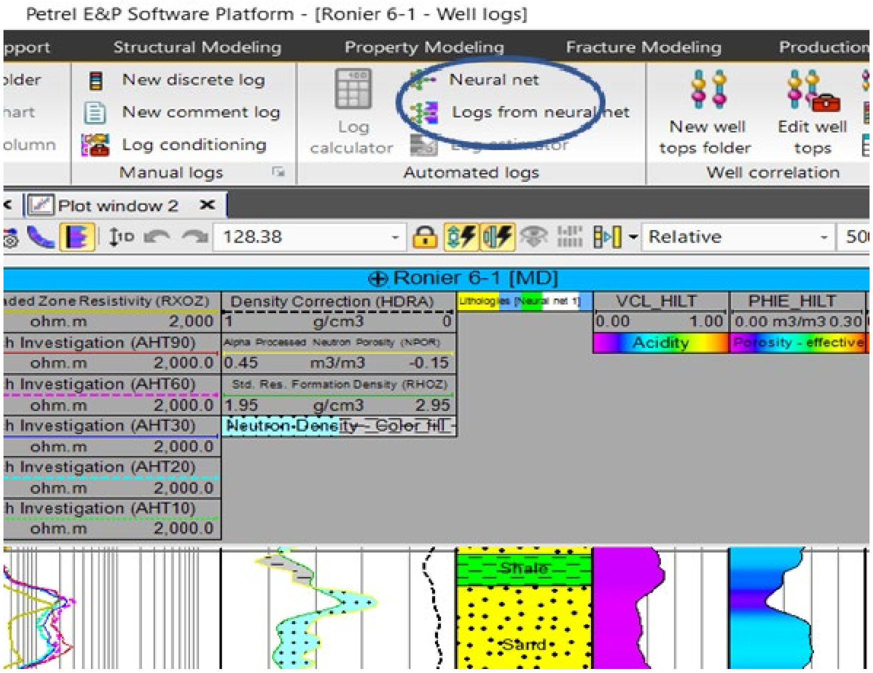

Figure 4. Schlumberger Petrel's Neural Net functionality.

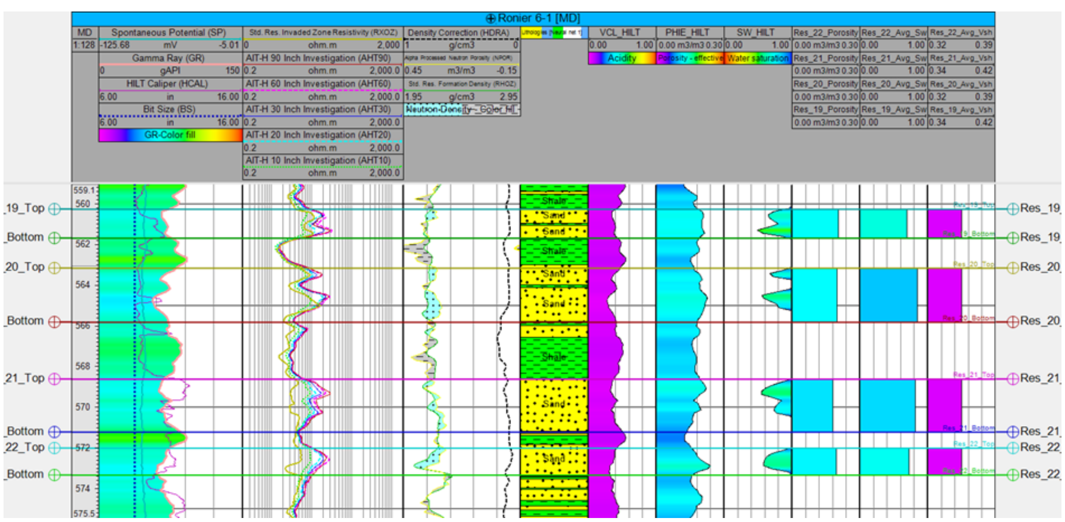

Figure 5. Cross-section showing the average porosity, water saturation and shale volume calculated for Reservoirs 19, 20, 21, 22.

3.2. Average water saturation, effective porosity, volume shale and hydrocarbon saturation

The availability of a wide range of logs enabled the rapid determination of these various parameters without direct recourse to the empirical formulas typically used for this purpose.

The SW_HILT, PHIE_HILT, and VCL_HILT logs provided, respectively, water saturation, effective porosity, and clay volume percentage for each geological layer. These logs were subsequently used to calculate the arithmetic mean of each of these parameters for each reservoir (Figure 5). Regarding hydrocarbon saturation (S_h), it was inferred from water saturation (S_w) using the formula: $S_h = 1 - S_w$.

Table 1. Vsh and porosity classification [26-27]

V_{sh} (%)	Classification (V_{sh})	Porosity (%)	Classification ($Ø_{eff}$)
<5	Sand	<5	Negligible
5–15	Moderately shaly sand	6–10	Poor
15–25	Shaly sand	11–15	Fair
25–35	Very shaly sand	16–20	Good
>35	shale	21–25	Very good
		>25	Excellent

3.3. Irreducible water saturation (S_{wirr})

The Buckles method [28] was employed to determine the irreducible water saturation. Initially, the Buckles number (KBUCKL) was calculated using the formula:

$$KBUCKL = Ø_{eff} * S_w \qquad (1)$$

where $Ø_{eff}$: effective porosity; S_w: water saturation.

Once the Buckles number was obtained, the irreducible water saturation (Swirr) was calculated using the formula:

$$S_{wirr} = \min\,(1.00,\ S_w,\ KBUCKL/[Ø_{eff}\,/(1 - Vsh)]) \qquad (2)$$

where Vsh: volume shale.

It is important to note that if Swirr is greater than Sw, then the Buckles number used is incorrect.

3.4. Permeability (K)

In the absence of core analysis data, the following formula was used to calculate the permeability of each reservoir (reference):

$$K = C * Ø_{eff}^{\ D} / S_{wirr}^{\ E} \qquad (3)$$

where K: permeability, in millidarcies; C: permeability constant; D: porosity exponent; E: irreducible saturation exponent; $Ø_{eff}$: effective porosity; S_{wirr}: irreducible water saturation.

The preceding formula [28] was numerically applied using the following parameters: C = 3400 (in oil-bearing reservoirs); C = 340 (in gas-bearing reservoirs); D = 4.4; E = 2.0.

4. Results and discussion

Interpreted well logs are used to delineate physical rock characteristics like porosity, volume of shale, lithology [29]. Table 1 is used to describe the reservoir’s petrophysical properties. Log analysis of the Ronier 6-1 well has identified 31 zones of interest that are potential hydrocarbon reservoirs. The thicknesses of these potential hydrocarbon reservoirs vary widely, from 1.32 m for Reservoir 22 to 11.65 m for Reservoir 25. Reservoir 18 is the most porous, with an average porosity of 23% in the hydrocarbon zone. With an average porosity of around 14% in the hydrocarbon zone, Reservoirs 24 and 31 are the least porous (Table 2).

Average water saturation is lowest in reservoir 8, at around 45%. It is highest in reservoir 9, where it reaches 87%. Only reservoirs 3, 5, 8 and 10 have average water saturation levels below 60% (above which the risk of producing a large quantity of water about the hydrocarbons becomes very critical). Irreducible water saturation is above 30% in all reservoirs. It is highest in Reservoir 20, with an average value of around 54%, and lowest in Reservoir 8, with an average of around 30% (Table 2).

Table 2. Petrophysical parameters of Ronier 6-1 hydrocarbon reservoirs.

Dept (MD, m)	Reservoirs	Gross Pay Thickness	Average effective Porosity ($Ø_{eff}$)	Average Water Saturation (S_w)	Average Irreducible Water Saturation (S_{wirr})	Average Volume Shale (Vsh)	Average Permeability (K, mD)	Fluids	Reservoir Quality
314.35 - 318.33	Reservoir 1	3.98	0.17	0.61	0.45	0.26	0.69	Possible Gas	Poor
321.91 - 325.11	Reservoir 2	3.2	0.18	0.7	0.42	0.4	1.02	Possible Gas	Poor
333.91 - 336.61	Reservoir 3	2.7	0.2	0.54	0.35	0.36	23.93	Possible oil, gas	Fair
356.27 - 358.38	Reservoir 4	2.11	0.19	0.77	0.49	0.37	9.69	Possible oil, gas	Poor
359.90 - 363.00	Reservoir 5	3.1	0.19	0.53	0.33	0.38	21.12	Possible oil, gas	Fair
370.76 - 378.68	Reservoir 6	7.92	0.19	0.84	0.51	0.39	0.87	Possible gas	Poor
390.03 - 392.88	Reservoir 7	2.85	0.2	0.62	0.39	0.37	18.73	Possible oil, gas	Fair
395.09 - 397.15	Reservoir 8	2.06	0.2	0.45	0.30	0.33	31.44	Possible oil, gas	Fair
414.11 - 422.36	Reservoir 9	8.25	0.16	0.87	0.50	0.43	4.35	Possible oil, gas	Poor
428.02 - 431.90	Reservoir 10	3.88	0.19	0.51	0.33	0.36	21.40	Possible oil, gas	Fair
433.42 - 435.49	Reservoir 11	2.07	0.15	0.71	0.41	0.42	0.48	Possible gas	Poor
448.36 - 450.72	Reservoir 12	2.36	0.19	0.75	0.50	0.33	0.90	Possible gas	Poor
461.48 - 468.07	Reservoir 13	6.59	0.16	0.86	0.53	0.38	0.38	Possible gas	Poor
472.79 - 474.60	Reservoir 14	1.81	0.17	0.65	0.40	0.39	0.89	Possible gas	Poor
487.33 - 488.95	Reservoir 15	1.62	0.15	0.82	0.44	0.46	0.41	Possible gas	Poor
516.42 - 518.05	Reservoir 16	1.63	0.17	0.73	0.44	0.4	0.73	Possible gas	Poor
524.39 - 528.51	Reservoir 17	4.12	0.16	0.76	0.48	0.37	0.47	Possible gas	Poor
543.75 - 545.42	Reservoir 18	1.67	0.23	0.74	0.50	0.33	2.15	Possible gas	Poor
560.26 - 561.69	Reservoir 19	1.43	0.2	0.69	0.43	0.38	15.61	Possible oil	Poor
563.16 - 565.81	Reservoir 20	2.65	0.2	0.85	0.54	0.36	9.66	Possible oil, gas	Poor
568.62 - 571.22	Reservoir 21	2.6	0.18	0.82	0.51	0.38	6.95	Possible oil	Poor
572.01 - 573.33	Reservoir 22	1.32	0.19	0.73	0.47	0.35	10.13	Possible oil	Poor
593.78 - 595.50	Reservoir 23	1.72	0.18	0.72	0.47	0.35	8.21	Possible oil	Poor
612.01 - 617.61	Reservoir 24	5.6	0.19	0.74	0.50	0.33	9.28	Possible oil, gas	Poor
652.65 - 664.30	Reservoir 25	11.65	0.19	0.76	0.49	0.36	9.64	Possible oil, gas	Fair
671.87 - 673.05	Reservoir 26	1.18	0.18	0.7	0.44	0.37	0.92	Possible oil	Poor
840.43 - 844.36	Reservoir 27	3.93	0.2	0.72	0.43	0.34	0.75	Gas	Poor
849.27 - 851.04	Reservoir 28	1.77	0.19	0.73	0.48	0.36	1.27	Gas	Poor
1230.63 - 1232.84	Reservoir 29	2.21	0.14	0.74	0.47	0.44	1.04	Gas	Poor
1299.68 - 1302.43	Reservoir 30	2.75	0.16	0.65	0.41	0.37	3.46	Possible oil, gas	Poor
1378.89 - 1380.47	Reservoir 31	1.58	0.14	0.63	0.41	0.36	0.64	Gas	Poor

All potential reservoirs have an average shale content of over 30%, except reservoir 1, which has an average shale content of 26%. These average shale contents range from 26% in reservoir 1 to 46% in Reservoir 15. Reservoirs 3, 5, 8, 10 and 18 are the only ones with an average permeability estimated at over 20 mD. Reservoir 8 has the highest permeability, with a value of around 31.44 mD, while reservoir 13 is the least permeable, with an estimated permeability of around 0.38 mD (Table 2). Based on the results of the log analysis of the Ronier 6-1 well, only Reservoirs 3, 5, 8,10 and 25 could be qualified as fair, while the others all show low or very low potential (Table 2).

Reservoirs 1, 2 and 3 are all very shaly sands (Table 1) with more than 30% shale. The interest of these reservoirs lies in the fact that over much of their hydrocarbon zones, minimum water saturations are below 60%. The minimum water saturation for reservoir 1 is 42% that for reservoir 2 is 55%, while that for reservoir 3 is 37%. The discrepancy between the Rxo (resistivity of the invaded zone) and AHT 90 (resistivity of the uninvaded zone) values suggests the presence of gas in reservoirs 1 and 2, while in reservoir 3, it could indicate the presence of gas in the upper part, and oil in the lower (Figure 6).

Like the three Reservoirs mentioned above, Reservoirs 4, 5 and 6 are very shaly sands (Table 1), with the percentage of shale being minimal in Reservoir 6 (around 25%). The figure 6 shows the very low hydrocarbon saturation in Reservoirs 4 and 6, and a fairly good hydrocarbon saturation in Reservoir 5. In fact, the average hydrocarbon saturation (deducted from the water saturation log) is around 47%, with the maximum saturation being around 63%; this increases the interest in this Reservoir. Analysis of the resistivity logs suggests the presence of gas in the upper part of the hydrocarbon zone, and oil in the lower part, for Reservoirs 4 and 5. On the other hand, these logs only reveal signs of gas in Reservoir 6.

The minimum shale content in sandy Reservoirs 7, 8 and 9 is 32%, 30% and 34% respectively (Table 2). While Reservoirs 7 and 8 have fair hydrocarbon saturations, Reservoir 9 has some hydrocarbon saturation peaks, but a low overall average hydrocarbon saturation. Slight offsets between the Neutron (NPOR) and Density (ROHZ) logs in the hydrocarbon zones could indicate the presence of oil, while more pronounced offsets would suggest the presence of gas. The analysis of those logs, suggests the possible presence of oil and gas in Reservoirs 7, 8 and 9 (Figure 6).

Reservoirs 10, 11 and 12 are very shaly sands with minimum shale contents of around 30%, 35% and 29%, respectively. While it is true that Reservoir 12 has a low hydrocarbon saturation, Reservoirs 11 and 10 have fair and fairly good hydrocarbon saturations, respectively. Reservoir 10 has a thicker hydrocarbon zone (approx. 3.88 m), with a maximum hydrocarbon saturation of up to 65% (Figure 6), compared with 53% for Reservoir 11, whose hydrocarbon zone is almost 1.5 m thick (Table 2). While the presence of oil and gas (mostly gas) is expected in Reservoir 10, the discrepancy between the Neutron and Density logs suggests an exclusive presence of gas in Reservoir 11 (Figure 6). As for Reservoir 12, the Neutron and Density logs reveal the presence of gas and no oil (Figure 7).

Reservoirs 13, 14 and 15 are very shaly sands with shale content over 28%. Among those reservoirs, only Reservoir 14 has a maximum hydrocarbon saturation of over 50%, with an average of 35% (Figure 7). The large discrepancies between Neutron and Density logs reveal a predominant presence of gas in those different reservoirs. It is also important to note the high Caliper values compared to the bit diameter (Figure 7), indicating the presence of significant caving in that section of the well (particularly in Reservoirs 13 and 14). That caving certainly had affected the recordings made in that section, reducing their quality, and the reliability of the interpretation that can be made.

Reservoirs 16, 17 and 18 have minimum shale contents of 30% (Table 2); they are also very shaly sands. Neutron and density log analysis in their hydrocarbon zone reveals the presence of mainly gas. However, as with Reservoirs 13, 14 and 15, the high caliper values compared to the drill bit diameter indicate the presence of caving (Figure 7), which has considerably reduced the quality of the logs, thus also affecting the reliability of the interpretation.

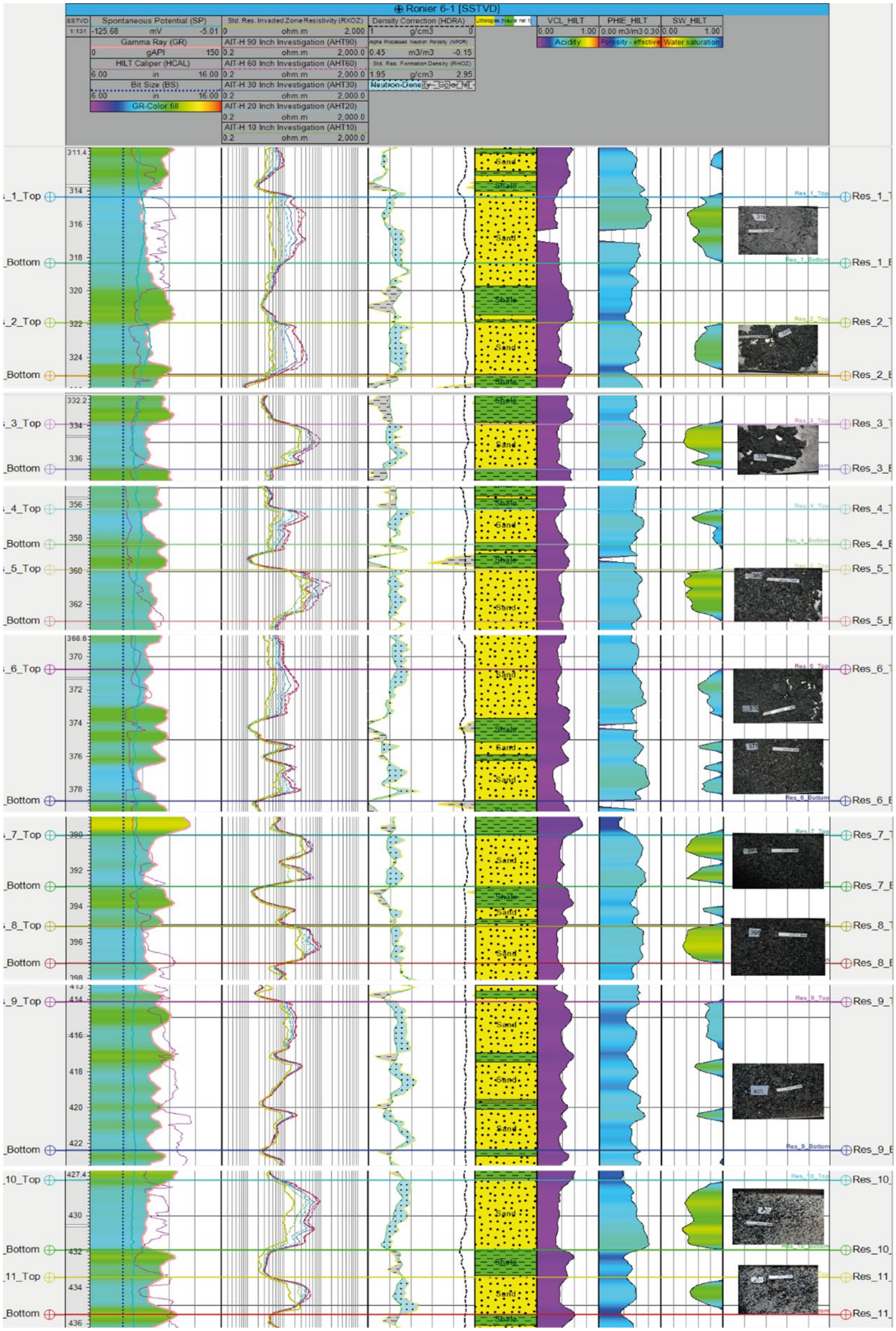

Figure 6. Ronier 6-1 well logs showing Reservoirs 1 to 11.

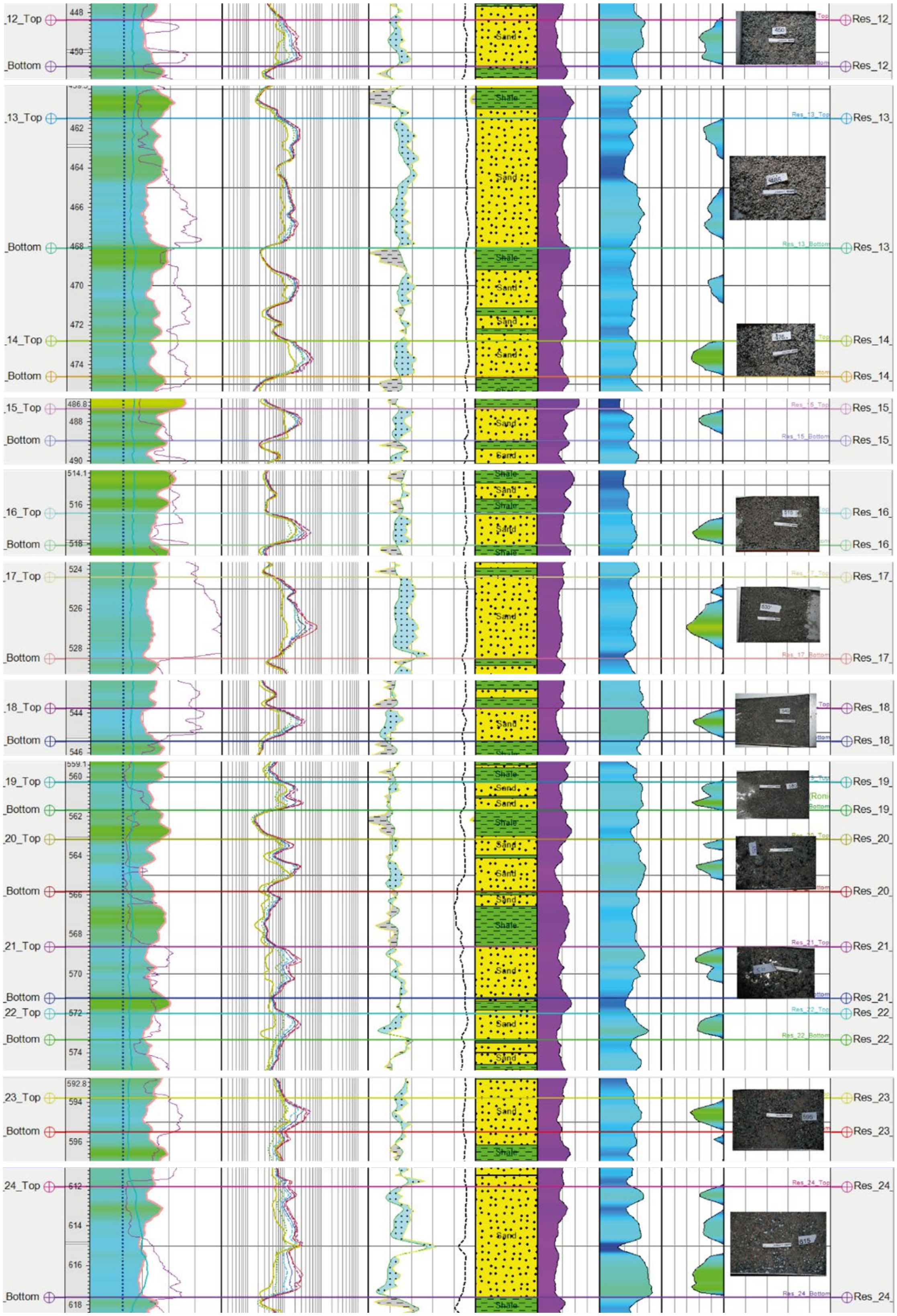

Figure 7. Ronier 6-1 well logs showing Reservoirs 12 to 24.

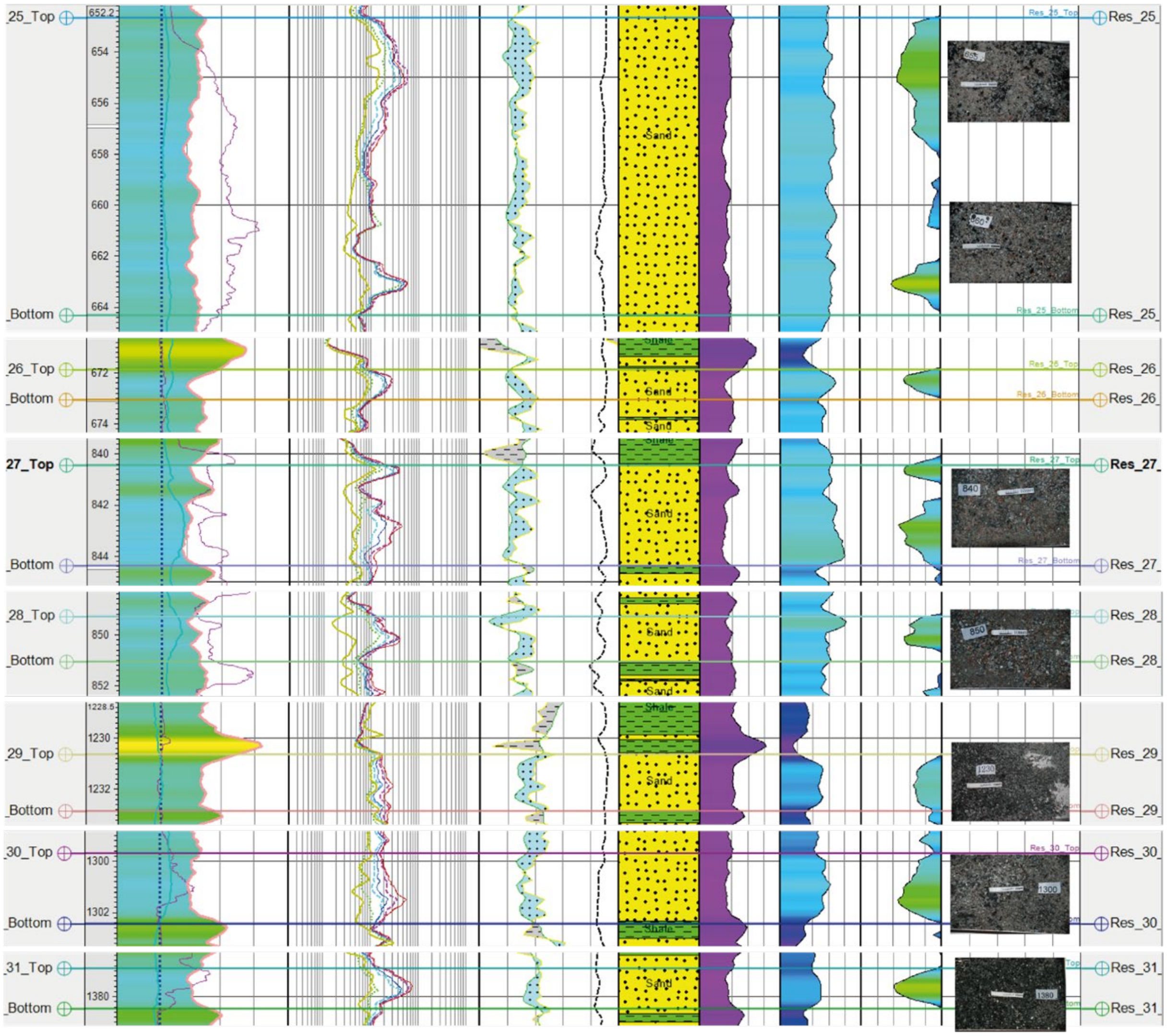

Figure 8. Ronier 6-1 well logs showing Reservoirs 25 to 31.

Reservoirs 19, 20, 21 and 22 are also very shaly sands, with minimum shale contents of over 25% (Table 2). Neutron and density logs suggest the presence of oil in Reservoirs 19, in the upper part of Reservoir 20, and in Reservoirs 21 and 22. The offset between neutron and density logs near the base of Reservoir 20 indicates the presence of gas (Figure 7). This fluid pattern in Reservoir 20 may be because the reservoir has thin layers of impermeable shale between the sand layers. Although showing some peaks, hydrocarbon contents in these reservoirs are low and of little interest.

Reservoirs 23 and 24 are very shaly sands containing at least 27% shale (Table 2). Reservoir 23 has a localised peak in hydrocarbon saturation, while Reservoir 24 has three slightly wider, more widespread peaks. The most interesting hydrocarbon zone in Reservoir 24 is at its base, with a maximum saturation of 51% (Figure 7). While analysis of the density and neutron logs would suggest a predominant presence of oil in Reservoir 23 and the lower part of Reservoir 24, they predict a predominant presence of gas in the upper part of Reservoir 24. It would also be important to note the presence of caving over 4 inches in this Reservoir, reducing the quality and reliability of the data.

With at least 28% of shales, Reservoirs 25 and 26 are very shaly sands (table 1), just like the previous reservoirs identified. Reservoir 25, whose zone of interest is around 11 m thick (Table 2), shows good hydrocarbon saturation at its base (up to 54%) and top (around 62% at its peak), with very low values in the middle (less than 18%). Analysis of the resistivity, neutron and density logs reveal signs of oil and gas in the upper part of Reservoir 25, with a contact zone at around 655 m. At the base of the reservoir, the density and neutron logs (Figure 7) suggest the presence of mainly oil. As for Reservoir 26, whose hydrocarbon saturation peak (around 47%) is localised, we would more likely expect to find oil. Also noteworthy is the caving over the entire thickness of the zone of interest in Reservoir 25, which calls for caution when interpreting.

Reservoirs 27 and 28 are very shaly sands containing more than 27% of shales (Table 2). The hydrocarbon zone in Reservoir 27 fills almost its entire thickness, while that in Reservoir 28 is around 1 m thick. The maximum oil saturation in Reservoir 27 is 54%, and the neutron and density logs (Figure 8) suggest the presence of mainly gas. As for Reservoir 28, the hydrocarbon saturation (essentially gas) reaches around 47%.

Reservoirs 29, 30 and 31, like the previous reservoirs, are very shaly sands and contain at least 32% of shales (Table 2). Their maximum hydrocarbon saturations are around 36%, 54% and 59% respectively. Reservoirs 29 and 31 are expected to contain mainly gas, while Reservoir 30 is expected to contain a mixture of oil and gas.

4.1. Promising hydrocarbon reservoirs

Reservoirs 3, 5, 7, 8, 10 and 25 are the only reservoirs found with a fair quality. Figure 9 shows that those reservoirs are mostly sandstones. Their hydrocarbon saturations vary from 24% in Reservoir 25 to 55% in Reservoir 8 (Table 3). Reservoir 25 is the only promising reservoir with a hydrocarbon saturation less than 38%.

Figure 10 shows that in Reservoirs 3, 5, 8, and 10, the hydrocarbon saturation is higher than the irreducible water saturation. However, the opposite is true in Reservoirs 7, and 25. In Reservoir 25, the irreducible water saturation is almost twice as much as the hydrocarbons. That high irreducible water saturation could make it harder to extract the hydrocarbons. When designing and selecting hydrocarbon recovery techniques, it is important to consider where the hydrocarbon zones are located, especially when deciding where to make the perforations. Additionally, the difference in irreducible water and hydrocarbon saturations in Reservoirs 7 and 25 might be because their respective gross pay thicknesses were much higher than their respective net pay thicknesses (Figure 11), since we used the gross pay thickness to calculate the fluids saturation. This also explains the low average hydrocarbon saturation in Reservoir 25. However, its configuration (Figure 8), and high net pay thickness of about 6.15 m (Table 3) make it a promising hydrocarbon reservoir.

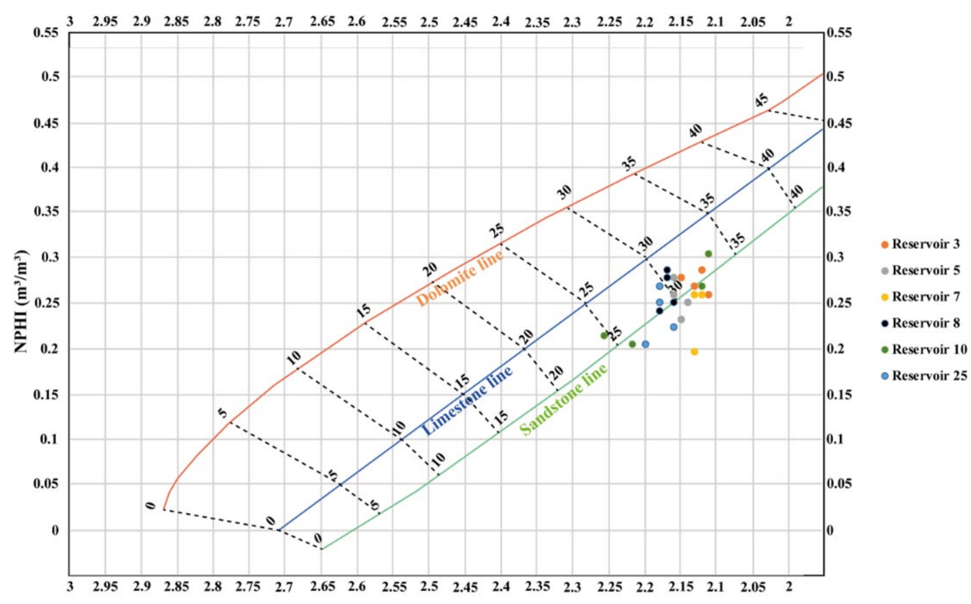

Figure 9. Density-Neutron plot for lithology identification.

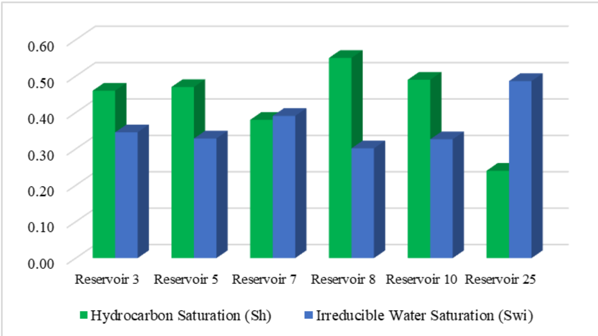

Figure 10. Comparison between hydrocarbon saturation and irreducible water saturation.

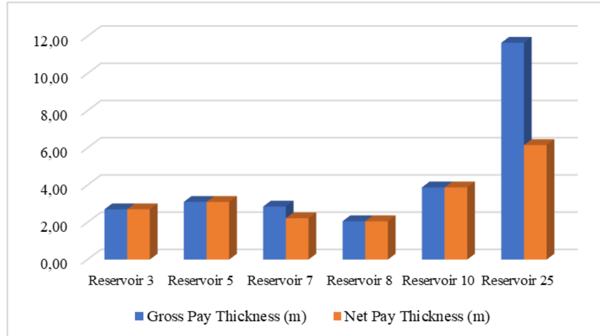

Figure 11. Comparison between gross and net pay thickness.

Table 3. Petrophysical properties of Ronier 6-1's promising reservoirs.

	Water saturation (S_w)	Hydrocarbon saturation (S_h)	Irreducible water saturation (S_{wirr})	Gross pay thickness (m)	Net pay thickness (m)	Effective porosity ($Ø_{eff}$)	Permeability (K, mD)	Fluids
Reservoir 3	0,54	0,46	0,35	2,70	2,70	0,2	23,93	Possible oil, gas
Reservoir 5	0,53	0,47	0,33	3,10	3,10	0,19	21,12	Possible oil, gas
Reservoir 7	0,62	0,38	0,39	2,85	2,22	0,2	18,73	Possible oil, gas
Reservoir 8	0,45	0,55	0,30	2,06	2,06	0,2	31,44	Possible oil, gas
Reservoir 10	0,51	0,49	0,33	3,88	3,88	0,19	21,40	Possible oil, gas
Reservoir 25	0,76	0,24	0,49	11,65	6,15	0,19	9,64	Possible oil, gas

5. Conclusion

The detailed analysis of the Ronier 6-1 well logs helped identify several hydrocarbon reservoirs, but those reservoirs are mostly poor. Only six out of the 31 reservoirs identified are classified as fair, and none as a good reservoir. Many caving occurred during the drilling processes, having a negative effect on the well log data recorded in many reservoirs like the Reservoir 25. The interpretation made for those reservoirs should be considered with caution, and additional studies should be run (like core analysis) to adjust and improve the reliability of the interpretation. All the reservoirs are very shaly sand reservoirs, but the six ones qualified as fair have good porosity and permeability values. Their hydrocarbon saturation varies from 24% in Reservoir 25 to 55% in Reservoir 8. Reservoir 25 has been considered interesting due to its net pay thickness (about 6.15 m). Adding core analysis data will considerably improve the precision of the study.

Acknowledgement

This paper is part of the doctoral work of the first author, who is grateful to the African Union and the Pan-African University, Life and Earth Sciences, University of Ibadan, Nigeria for awarding this fellowship. The authors also thank the anonymous reviewers for their helpful comments, suggestions and thoughtful criticisms, which have significantly improved the quality of this paper.

Funding and conflict of interest

The African Union Commission funded this work through the Pan African University, Life and Earth Sciences Institute (Including Health and Agriculture), Ibadan, Nigeria.
The authors have no competing interests to declare relevant to this article's content.

References

[1] Dou L, Kunye X, and Jingchun W. Geological Features of Hydrocarbon Reservoirs of Bongor Basins, 2023; 299-378.
[2] Genik GJ. Regional framework, structural and petroleum aspects of rift basins in Niger, Chad and the Central African Republic (C.A.R.). Tectonophysics, 1992; 213: 169–185.
[3] Dou L, Xiao K, Hu Y, Song H, Cheng D, and Du Y. Petroleum geology and a model of hydrocarbon accumulations in the Bongor Basin, the republic of Chad. Acta Pet. Sin., 2011; 32 (3): 379–386. (In Chinese With English Abstract)
[4] Lirong D, Kunye X, and Jingchun W. Regional Geological Characteristics Bongor Basins of the Central African Rift System, 2023; 25-67.
[5] Fagbemi OI, Olayinka AI, Oladunjoye MA, and Edigbue PI. Focused reservoir characterization: analysis of selected sand units using well log and 3-D seismic data in 'Kukih' field, Onshore Niger Delta, Nigeria. Scientific Reports, 2024; 14(1): 13763.
[6] Rider MH. The Geological Interpretation of Well Logs 2nd edn, 2002; 133–147 (Whittles Publishing, Dunbeath).
[7] Song H, and Dou L. An exploratory research on geological conditions of hydrocarbon pooling and distribution patterns of reservoirs in the Bongor Basin. Oil Gas Geol., 2009; 30(6): 762–767.
[8] Eyike, A., Werner, S.C., Ebbing, J. and Dicoum, E.M. (2010) On the Use of Global Potential Field Models for Regional Interpretation of the West and Central African Rift System. Tectonophysics, 492, 25-39. https://doi.org/10.1016/j.tecto.2010.04.026
[9] Dai S, Wang W, Chen Z, Luo M, Yang S, Liu C, and Zhang Y. Application of slope break controlled deposition theory in oil and gas exploration in Bongor Basin, Chad. Oil Geophysical Prospecting, 2010; 45(3): 448-453. (in Chinese with English abstract).
[10] Shellnutt JG, Lee TY, Yang CC, Hu ST, Wu JC, Wang KL, and Lo CH. Late Permian mafic rocks identified within the Doba basin of southern Chad and their relationship to the boundary of the Saharan Metacraton. Geological Magazine, 2015; 152(6): 1073-1084.
[11] Zhao J, Tong X, Xiao K, Dou L, Ji H, Du Y, Yuan Z and Xiao G. Sedimentary diagenetic characteristics of Reservoir sandstone and their controlling factors in Bongor Basin. Chad. Jilin Daxue Xuebao, 2013; 43(3): 649-658 (in Chinese with English abstract).
[12] Chen Z, Liu L, Bian D, Dou L, Huang X, and Xiao K. Diagenetic evolution and characteristics of the Lower Cretaceous clastic reservoir of B Basin, South Chad. 2006.
[13] Guiraud R, Bellion Y, Benkhelil J, and Moreau C. Post-hercynian tectonics in northern and western Africa. Geol. J., 2010; 22(22): 433–466.
[14] Lowell JD and Uenik UJ. Sea floor spreading and structural evolution of Lower Cretaceous sublacustrine fan in BN block of BG Basin, Central Africa. Lithol. Reserv., 1972; 28(3): 86-94, 126. (in Chinese with English abstract).
[15] Makris J, and Rihm R. Shear-controlled evolution of the Red Sea: pull apart model. Tectonophysics, 1991; 198(2–4): 441–466. https://doi.org/10.1016/00401951(91)90166-p
[16] Dou LR, Wei XD, Wang JC, Li JL, Wang RC, and Zhang SH. Characteristics of granitic basement reservoir in Bongor Basin. Acta Petrolei Sinica, 2015; 36(8): 898–903.
[17] Zhang M, Song B, Tian Z, Zhang N, Shi Y and Wang Q. Basement lithology characteristics and forming age of Bongor Basin Chad. Open J. Nat. Sci., 2016; 4(1): 63-80 (in Chinese with English abstract).
[18] Tan M, Zhu X, Geng M, Zhu S, and Liu W. The occurrence and transformation of lacustrine sediment gravity flow related to depositional variation and paleoclimate in the Lower Cretaceous Prosopis Formation of the Bongor Basin, Chad. Journal of African Earth Sciences, 2017; 134: 134–148. https://doi.org/10.1016/j.jafrearsci.2017.06.003
[19] Petters SW and Ekweozor CM. Petroleum Geology of the Benue Trough and Southeastern Chad Basin, Nigeria. American Association of Petroleum Geologists Bulletin, 1982; 66: 1141-1149.
[20] Fairhead JD. Mesozoic Plate Tectonic Reconstructions of the Central South Atlantic Ocean: The Role of the West and Central African Rift System. Tectonophysics, 1988; 155: 181-191. http://dx.doi.org/10.1016/0040-1951(88)90265-X
[21] Dou L, Li W, and Cheng D. Hydrocarbon accumulation period and process in Baobab area of Bongor Basin. Journal of African Earth Sciences, 2020; 161: 103673. https://doi.org/10.1016/j.jafrearsci.2019.103673
[22] Dou L, Xiao K, Wang J, Liu B, Pan X, and Wan L. Petroleum geology and exploration practice of strongly-inverted rift basin. Beijing: Petroleum Industry Press, 2018.

[23] Dou L, Wang J, Wang R, Wei X, and Shrivastava C. Precambrian basement reservoirs: Case study from the northern Bongor Basin, the Republic of Chad. AAPG Bulletin, 2018; 102(09): 1803–1824. https://doi.org/10.1306/02061817090
[24] Xiao KY, Zhao J, Yu ZY, Sheng YM, Hu Y, Yuan ZY, Hou FD and Zhang GL. Structural characteristics of intensively inversed Bongor Basin in CAR and their impacts on hydrocarbon accumulation. Earth Science Frontiers, 2014; 21(3): 172-180.
[25] Suhail H, Yuan X, Li J, Liu H, Liu Y, and Ma C. Paleostress Reconstruction from 3D Seismic Data and Slip Tendency in the Northern Slope Area of the Bongor Basin, Southwestern Chad. Open Journal of Geology, 2023; 13: 536-578. https://doi.org/10.4236/ojg.2023.135024
[26] Adagunodo TA, Bayowa OG, Alatise OE, Oshonaiye AO, Adewoyin OO, and Opadele VO. Characterization of reservoirs and depositional study of J-P Field, shallow offshore of Niger Delta Basin, Nigeria. Scientific African, 2021; 15: e01064. https://doi.org/10.1016/j.sciaf.2021.e01064
[27] Metwalli FI, Shendi EH, Fagelnour MS. Core and well logs interpretation for better reservoir characterization in Shushan Basin. Egypt. Arabian J. Geosci. 14, 2587. model. Tectonophysics, 2021; 198: 441 – 468.
[28] Timur A. An Investigation of Permeability, Porosity and Residual Water Saturation Relationships for Sandstone Reservoirs. The Log Analyst, 1968; 9: 3-5.
[29] Ayodele F, John A, Florence O. Seismic and Petrophysical Characterization of Subsurface Reservoirs within Arike Field, Niger Delta, Nigeria. Petroleum and Coal, 2023; 65 (2): 505 – 518.

To whom correspondence should be addressed: Mahamat Choukou Mahamat, Pan African University, Institute of Life and Earth Sciences Institute (Including Health and Agriculture), Ibadan, Oyo State, Nigeria,
E-mail: *machoukou1991@gmail.com*